



HAL
open science

Direct Enthalpy Measurement for Hydrogenation of Liquid Organic Hydrogen Carriers by Differential Scanning Calorimetry under H₂ Pressure

Florian d'Ambra, Vicent Fauchaux, Emmanuel Nicolas, Thibault Cantat, Gérard Gébel, Parviz Hajiyev

► **To cite this version:**

Florian d'Ambra, Vicent Fauchaux, Emmanuel Nicolas, Thibault Cantat, Gérard Gébel, et al.. Direct Enthalpy Measurement for Hydrogenation of Liquid Organic Hydrogen Carriers by Differential Scanning Calorimetry under H₂ Pressure. *Industrial and engineering chemistry research*, 2024, 63 (30), pp.13157-13168. 10.1021/acs.iecr.4c01739 . hal-04681564

HAL Id: hal-04681564

<https://hal.science/hal-04681564v1>

Submitted on 29 Aug 2024

HAL is a multi-disciplinary open access archive for the deposit and dissemination of scientific research documents, whether they are published or not. The documents may come from teaching and research institutions in France or abroad, or from public or private research centers.

L'archive ouverte pluridisciplinaire **HAL**, est destinée au dépôt et à la diffusion de documents scientifiques de niveau recherche, publiés ou non, émanant des établissements d'enseignement et de recherche français ou étrangers, des laboratoires publics ou privés.



Distributed under a Creative Commons Attribution - NonCommercial - NoDerivatives 4.0 International License

Direct enthalpy measurement for hydrogenation of liquid organic hydrogen carriers by Differential Scanning Calorimetry under H₂ pressure

Authors:

Florian D'Ambra Univ. Grenoble Alpes, CEA, LITEN, F-38054 Grenoble, France

Vincent Faucheu Univ. Grenoble Alpes, CEA, LITEN, F-38054 Grenoble, France

Emmanuel Nicolas Université Paris-Saclay, CEA, CNRS, NIMBE, 91191 Gif-sur-Yvette, France

Thibault Cantat Université Paris-Saclay, CEA, CNRS, NIMBE, 91191 Gif-sur-Yvette, France

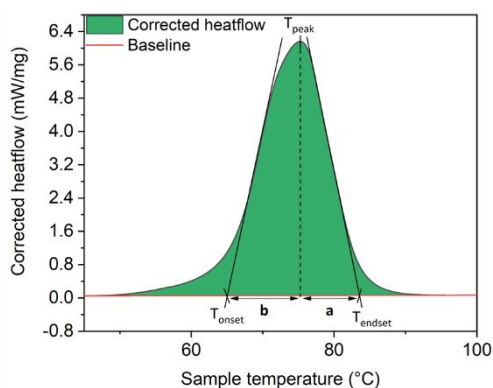
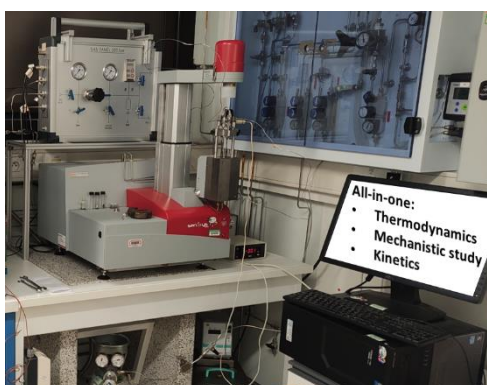
G rard G bel Univ. Grenoble Alpes, CEA, LITEN, F-38054 Grenoble, France

Parviz Hajiyev Univ. Grenoble Alpes, CEA, LITEN, F-38054 Grenoble, France. E-mail: parviz.hajiyev@cea.fr

Abstract

In this contribution, we report the hydrogenation enthalpy direct measurement of well-studied Liquid Organic Hydrogen Carriers (LOHC) (Dibenzyltoluene, N-Ethylcarbazole, 2-Octanone) and of a new LOHC (Acetophenone) by differential scanning calorimetry (DSC) under H₂ pressure. The obtained hydrogenation enthalpies showed good correlation with DFT predictions and the literature. Moreover, multistep hydrogenation processes were investigated, evidencing that transfer hydrogenation occurred during the reaction. The study of bifunctional LOHC such as acetophenone and its derivatives showcased the potential of direct enthalpy measurement for rapid LOHC screening. Besides, a DFT correction factor for this specific bifunctional LOHC class was experimentally obtained, enabling more precise DFT predictions for similar systems. Kinetic parameters such as the activation energies for the catalytic Ru/Al₂O₃ system were also determined to be in the 45-60 kJ/mol range, compatible with the H₂ adsorption on the Ru surface. The detrimental effect of steric hindrance was also observed. Finally, the reaction order in H₂ was experimentally estimated to ~1 for all of the studied LOHCs.

Graphical abstract



Highlights

- Direct LOHC hydrogenation enthalpy measurement by DSC under H₂ pressure.
- Enabling of rapid screening of new potential bifunctional LOHC systems.
- Mechanistic study of multistep hydrogenation processes.
- Correction of the liquid phase enthalpy DFT prediction by an experimental factor.

- Kinetic parameters (activation energy, reaction order) obtained from the same data.

Keywords

- DFT modelling
- DSC
- Hydrogenation
- LOHC (liquid organic hydrogen carrier)
- Enthalpy

Acronyms table

TERM	ACRONYM
1-Cyclohexylethanol	CHEA
1-Phenylethanol	PEO
Acetophenone	APO
Acetylcyclohexane	ACH
2-Octanone	2-OC
Dibenzyltoluene	DBT
N-Ethylcarbazole	NEC
Benzophenone	BPO
2-Methylacetophenone	2Me-APO
4-Methylacetophenone	4Me-APO
2,2,2-Trifluoroacetophenone	3F-APO
Activation energy	E_a
Degree of hydrogenation	DoH

Introduction

The implementation of low-carbon intermittent energies in our energy mixes necessitates the development of massive energy storage to accommodate for the upcoming offer-demand energy incompatibilities.^{1,2} One of the current envisioned solutions is based on the conversion of excess renewable energy into hydrogen (H₂). However, its low volumetric density in gaseous phase at normal conditions of temperature and pressure limits its large-scale deployment. Thus, facilitating H₂ storage has been a challenge over the past decades.³ The liquid organic hydrogen carrier (LOHC) technology stores and unloads H₂ through a cycle of hydrogenation and dehydrogenation catalytic reactions performed on a liquid organic framework that can easily and safely be stored and transported.⁴

One of the key parameters of the system is its reaction enthalpy that directly impacts the LOHC storage energy efficiency. Numerous studies aimed at reducing this enthalpy and most work in this direction was achieved by modelling the enthalpy of a LOHC couple by Density Functional Theory (DFT).^{5,6} However, direct experimental validation has been scarce as enthalpies of formation were usually derived from combustion calorimetry experiments.⁷ Direct reaction calorimetry was previously used to follow the hydrogenation of nitroaromatics and heteroaromatics as well as heterogeneously-catalyzed enantioselective hydrogenation,^{8,9} but no work was directly related to the LOHC technology. Calorimetry in combination with computational studies was mostly used to uncover phase change thermodynamics, and numerous articles published by the Verevkin group reported their properties such as the enthalpy of fusion, enthalpy of vaporization, enthalpy of combustion and heat capacity.^{10,11}

From this consideration, the development of a direct and accurate enthalpy measurement methodology is still required to this date. To address this shortcoming, we looked at similar hydrogen storage systems like metal hydrides. There, two main techniques were developed to measure the reaction enthalpy: Pressure Composition Temperature (PCT) with a Sieverts apparatus¹² and high-pressure Differential Scanning Calorimetry (DSC)^{13,14}.

PCT experiments consist in the estimation of the pressure equilibrium plateau for a given temperature by adding controlled small aliquots of H₂ to the system. This technique is widely used by the metal hydrides community as the sample preparation can easily be achieved in oxygen-free conditions.¹⁵ However, it presents some intrinsic limitations such as indirect enthalpy measurement, irreproducibility due to uncontrolled H₂ leaks, plateau hysteresis between hydrogenation and dehydrogenation as well as susceptibility to phase change due to volume modification.^{16,17} Hence, our conclusion is that this technique is not suitable for LOHC applications.

Conversely, Differential Scanning Calorimetry (DSC) under H₂ pressure was used to directly measure the reaction enthalpy of metal hydrides systems for both hydrogenation and dehydrogenation in static and dynamic temperature modes.^{13,14} The conclusion of these articles stated that “*Present results clearly demonstrate that a pressure DSC is available as a rapid and convenient experimental means for assessing hydrogen absorption and desorption properties of hydrogen storage materials*”.¹⁴ To our knowledge, no article reported the study of a LOHC system by pressure DSC for either the hydrogenation or the dehydrogenation.

So far, DSC was used to study the transfer hydrogenation from a metal hydride to a LOHC under He at atmospheric pressure in dynamic temperature mode.¹⁸ Another example reported the study of the hydrogenation enthalpy of nitroaromatics to aminoaromatics in isothermal conditions by DSC.¹⁹

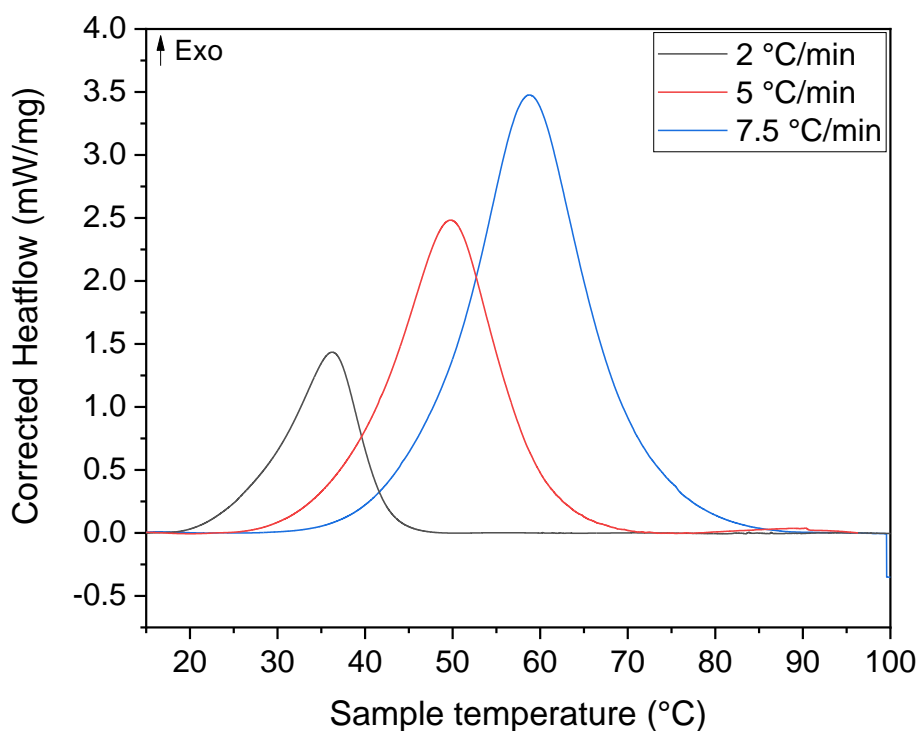
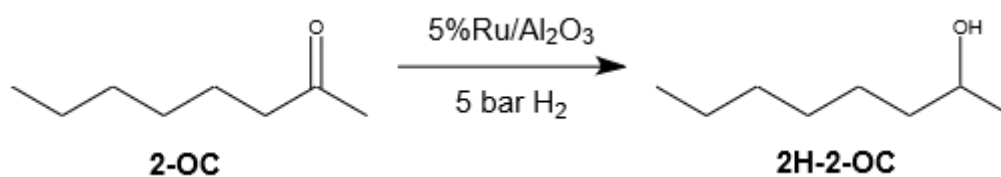
In this contribution, we propose to study different benchmark LOHC systems as well as new potential LOHC to assess their hydrogen adsorption properties by the H₂ pressure DSC

methodology in a dynamic temperature mode and to compare the obtained results with DFT calculations.

Results and discussion

- 1) Hydrogenation enthalpy measurement of state-of-the art LOHCs
 - a. 2-octanone (2-OC)

Hydrogenation enthalpy measurement by DSC was first tested with the conversion of 2-octanone to 2-octanol in presence of a 5%Ru/Al₂O₃ catalyst under 5 bar H₂. The corrected heat flow values divided by the LOHC weight at different heating rates are presented in Figure 1. The peak area for each heating rate as a function of the time (Figure S1 in the ESI) afforded the reaction enthalpy.



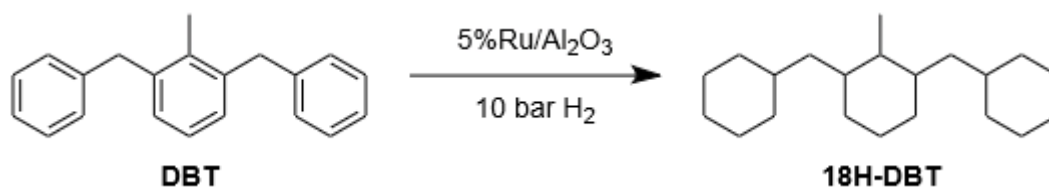
Heating rate (°C/min)	Degree of Hydrogenation	Enthalpy (kJ/mol H ₂)	Average enthalpy (kJ/mol H ₂)	DFT calculated enthalpy (kJ/mol H ₂)	Experimental gas phase enthalpy from the literature (kJ/mol H ₂)	Calculated liquid phase enthalpy from the literature (kJ/mol H ₂)
2	97%	-58.6	-59.2±2.0	-53.4	-52.97	-68.3±0.3
5	97%	-57.6				
7.5	98%	-61.5				

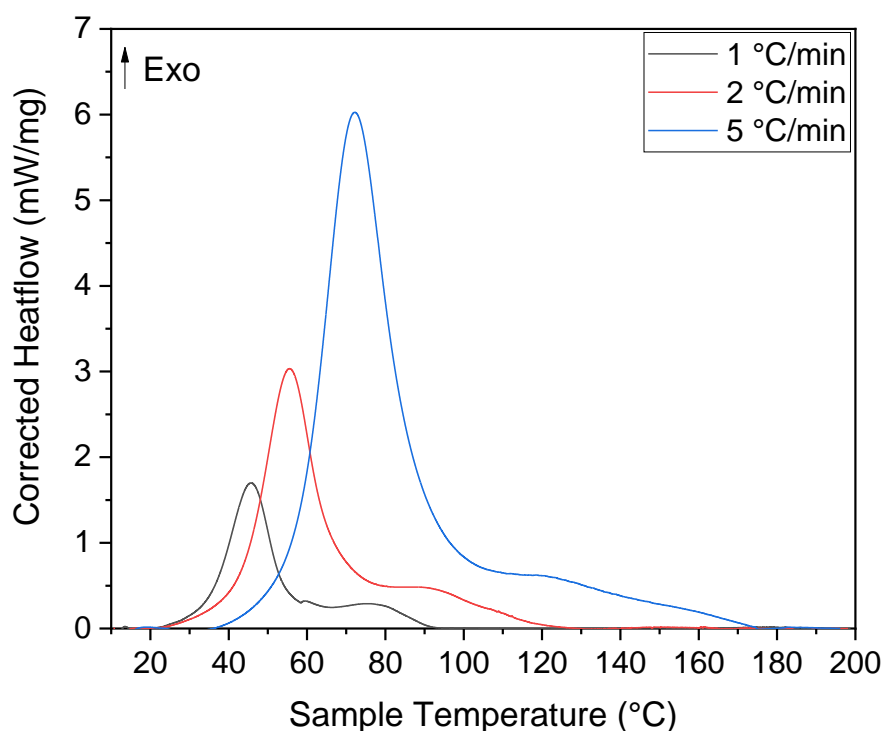
Figure 1 - Corrected heat flow values obtained for the DSC measurement of 2-octanone with 5%Ru/Al₂O₃ under 5 bar H₂ at different heating rates, derived hydrogenation enthalpy and its comparison with DFT calculated values and the literature.

A significant difference was noticed between our experimental and predicted values. Such gap was attributed to the limited accuracy of DFT calculations to model liquid phase interactions, in particular, in the presence of hydrogen bonds. Hence, our DFT enthalpy value was closely matching the experimental gas phase enthalpy value from the literature.²⁰ As the hydrogenation reaction occurred in liquid phase, the Hess law approach afforded a better approximation by using the vaporization enthalpies already reported in the literature.^{21,22} Nevertheless, this approximation did not perfectly match the DSC enthalpy value, possibly due to the cumulative errors or the partial evaporation of the LOHC, although no noticeable evaporation was observed due to a similar weight of the DSC system before and after the reaction and no endothermic peak was visible by DSC. Overall, the relative error between our DSC value and the liquid phase enthalpy is roughly 6.5%, which showcases the accuracy of the chosen characterization method. These relative error values are on-par with those of metal hydrides.¹⁵

b. Example of a liquid LOHC: Dibenzyltoluene (DBT)

Following these promising results, different state-of-the-art LOHCs were tested by the DSC method. Dibenzyltoluene (DBT) is one of the most studied LOHC in the literature and its hydrogenation enthalpy was reported as -71 kJ/mol H₂ derived from the calorimetric measurements of its enthalpies of combustion and vaporization.²³ Direct DSC hydrogenation at 10 bar H₂ in presence of 5%Ru/Al₂O₃ was performed. The DSC heat flow values presented two step hydrogenation process (a fused two-peak curve) as shown in Figure 2 and Figure S2 in the ESI.



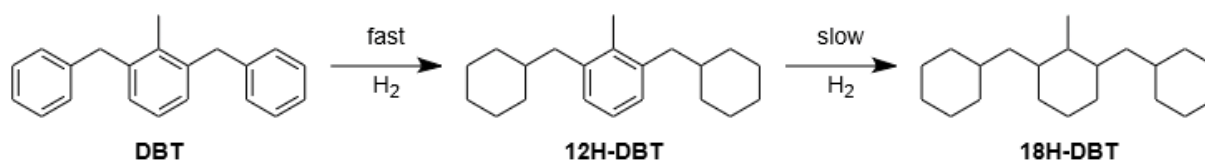


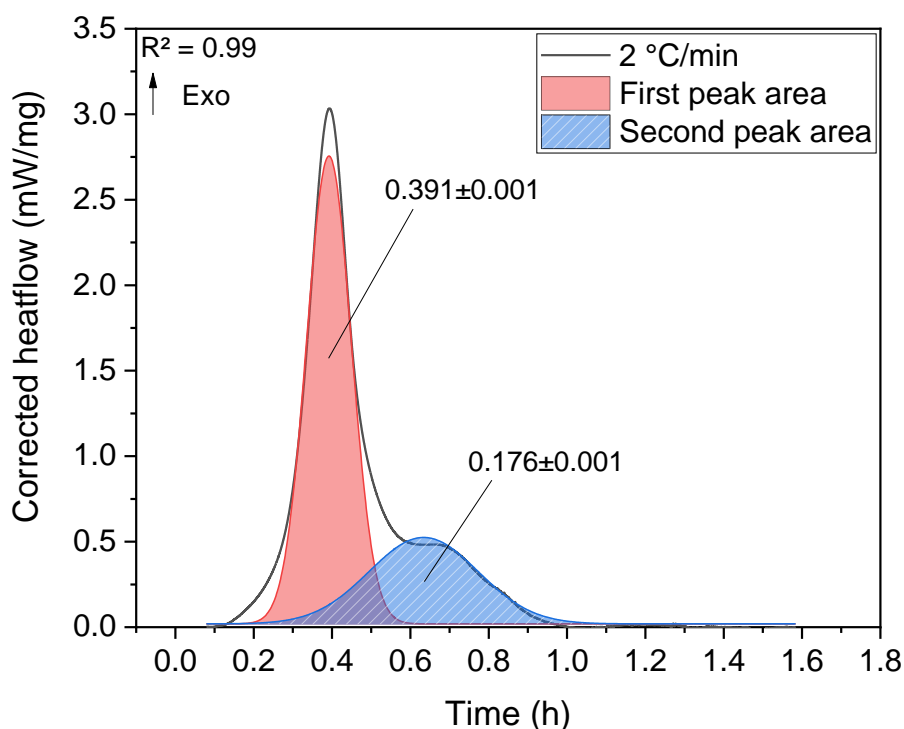
Heating rate (°C/min)	Degree of Hydrogenation	Enthalpy (kJ/mol H ₂)	Average enthalpy (kJ/mol H ₂)	DFT calculated enthalpy (kJ/mol H ₂)	Experimental liquid phase enthalpy from the literature (kJ/mol H ₂)
1	>99%	-70.2	68.9±1.4	-67	-71
2	>99%	-69.1			
5	>99%	-67.4			

Figure 2 - Corrected heat flow values obtained for the DSC measurement of dibenzyltoluene with 5%Ru/Al₂O₃ under 10 bar H₂ at different heating rates and their comparison with DFT calculated values and the literature.

The hydrogenation enthalpy was measured by simultaneously integrating both peaks, leading to an average enthalpy of -68.9 ± 1.4 kJ/mol H₂. This value was in good agreement with the previously reported hydrogenation enthalpy values (-71 kJ/mol H₂) and our own DFT calculated enthalpy value of -67 kJ/mol H₂, showing the applicability of the DSC and DFT approach for homocyclic LOHC systems.

In the literature, the hydrogenation kinetics of DBT were reported to first start on the external cycles before the internal cycle.²⁴ This is in good agreement with our double exothermic peak observation in DSC measurements. Thus, a peak deconvolution by Gaussian curve fitting was performed to verify this hypothesis. The area of each peak was obtained and their ratio was compared as presented in Figure 3 and Figure S3 in the ESI.





Heating rate (°C/min)	Peak 1 area (mWh/mg)	Peak 2 area (mWh/mg)	Peak 1/Peak 2 area ratio
1	0.376±0.001	0.151±0.002	2.490±0.040
2	0.391±0.001	0.176±0.001	2.222±0.020
5	0.410±0.001	0.196±0.004	2.092±0.049

Figure 3 - Peak deconvolution for Dibenzytoluene by gauss fitting (2°C/min heating rate), peak areas and ratio.

Assuming that a similar heat would be produced during the hydrogenation of any aromatic cycle, peak 1 was assigned to the heat produced by the hydrogenation of the two external rings while peak 2 was assigned to the heat produced by the hydrogenation of the internal ring. In this case, the peak area ratio should theoretically be equal to 2. Here, the peak area ratio values were close to 2, especially for higher heating rates. For lower heating rates, the increased ratio might be linked to the proton transfers between the external and internal rings of DBT. As a conclusion, the DSC method confirmed the DBT hydrogenation as a two-step process with visible transfer hydrogenation at lower heating rates. The influence of the temperature and/or kinetics on the transfer hydrogenation reaction was also exhibited, which might also pave the way to efficient design of transfer hydrogenation catalysts.

c. Example of a solid LOHC: N-Ethylcarbazole (NEC)

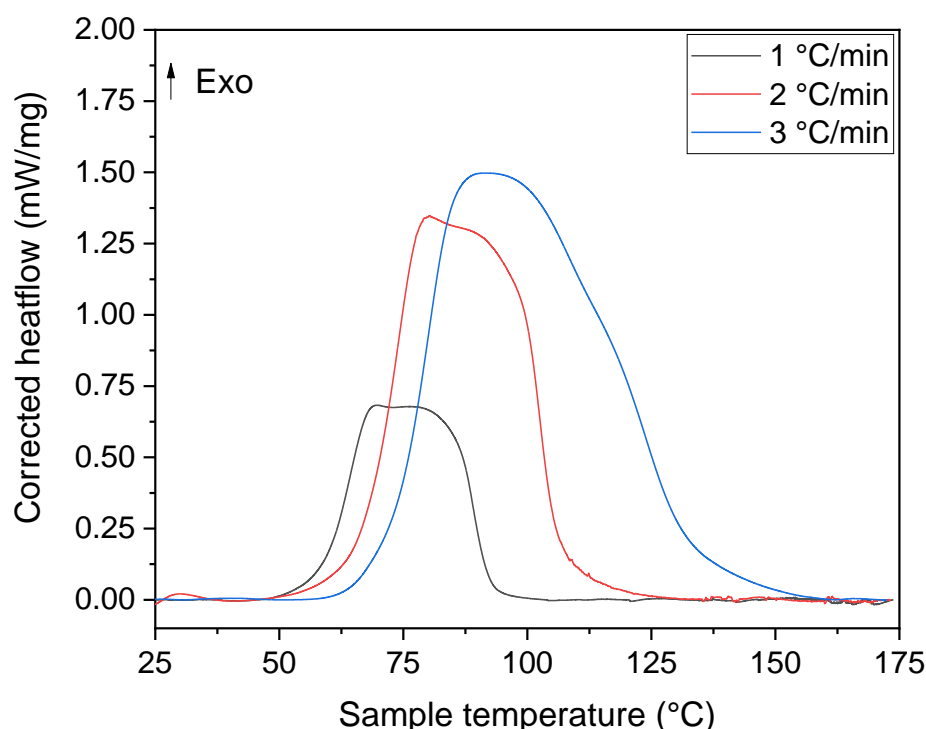
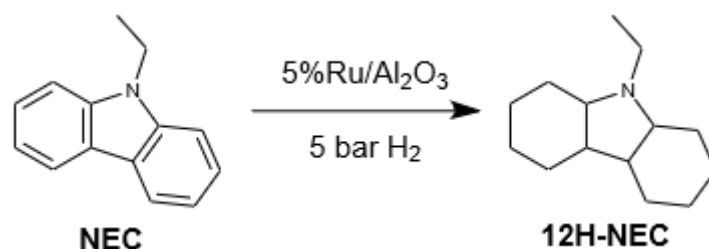
N-Ethylcarbazole is a LOHC that has the particularity of being solid at room temperature. However, as its enthalpy is advantageous (51 kJ/mol H₂) compared to the other state-of-the-art LOHC molecules and as its melting point is rather low (68 °C), NEC has been widely studied in the literature.⁵

However, its enthalpy measurement by DSC is incidentally complicated by its fusion. Indeed, the melting of a solid is usually an endothermic process while the hydrogenation of LOHC is exothermic. Hence, the separate evaluation of the fusion enthalpy is necessary to obtain an

accurate hydrogenation enthalpy value in the case of a partial overlap of both processes as it was observed in our case (see Figure S4 in the ESI).

Successive heating and cooling cycles under 5 bar N₂ were performed to obtain an enthalpy of fusion of 14.3 ± 0.2 kJ/mol (see Figure S5 in the ESI). This value was used for the calculation of the hydrogenation enthalpy (ΔH_{hyd}) as it was in good agreement with previous work reported in the literature: 15.10 ± 0.40 kJ/mol²⁵ and 16.55 ± 0.17 kJ/mol²⁶.

The combination of the hydrogenation and fusion enthalpies (ΔH_{comb}) was measured under an H₂ atmosphere. Then, the fusion enthalpy (ΔH_{fus}) was added to the obtained value as presented in Figure 4 and Figure S6 in the ESI.



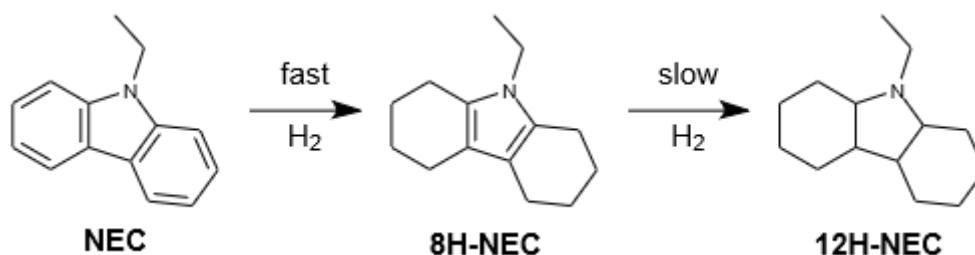
Heating rate (°C/min)	Degree of hydrogenation (DoH)	DoH-corrected ΔH_{comb} (kJ/mol H ₂)	Average measured ΔH_{comb} (kJ/mol H ₂)	Average measured ΔH_{fus} (kJ/mol H ₂)	Average measured ΔH_{hyd} (kJ/mol H ₂)	ΔH_{hyd} from DFT calculations (kJ/mol H ₂)	Experimental liquid phase ΔH_{hyd} from the literature (kJ/mol H ₂)
1	78%	-47.3	-46.9 ± 0.4	2.40 ± 0.03	-49.2 ± 0.4	-51.7	-51
2	73%	-46.8					
5	70%	-46.6					

Figure 4 - Corrected heat flow values obtained for the DSC measurement of N-ethylcarbazole with 5%Ru/Al₂O₃ under 5 bar H₂ at different heating rates, obtention of the hydrogenation enthalpy from the combined enthalpy

(ΔH_{comb}) and fusion enthalpy (ΔH_{fus}) and comparison with the hydrogenation enthalpy (ΔH_{hyd}) reported in the literature.

Here, the hydrogenation enthalpy value (-49.2 kJ/mol H₂) was in good agreement with our DFT calculations (-51.7 kJ/mol H₂) and the reported values in the literature (-51 kJ/mol H₂), highlighting the method applicability for solid LOHCs.

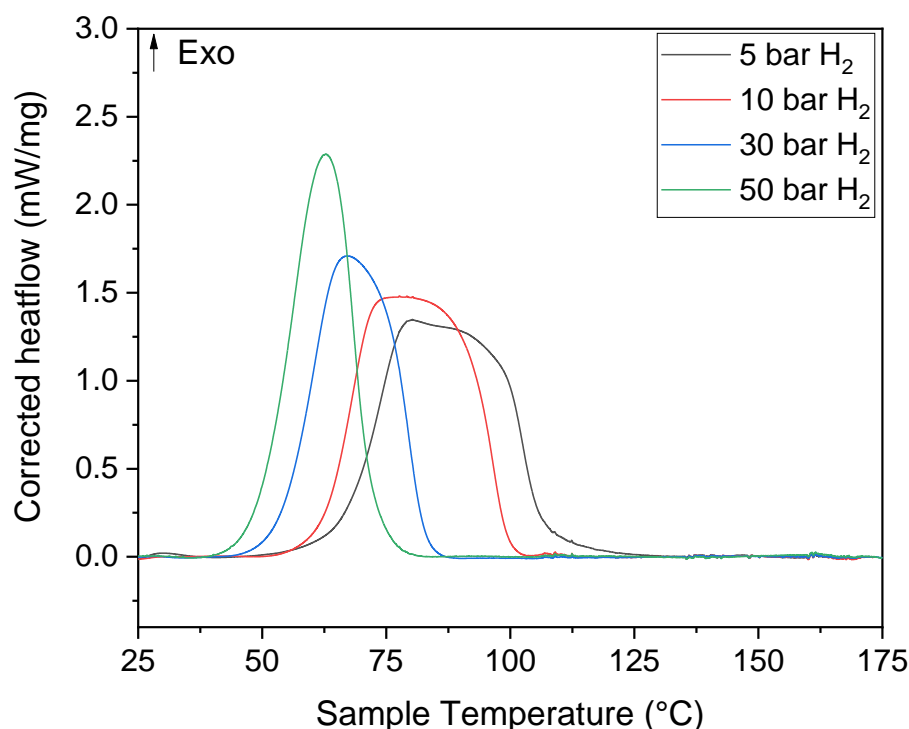
The DSC peak was broad, which might originate from a multistep process like previously presented for DBT. Indeed, similar to DBT, NEC hydrogenation was reported in the literature as a multistep process where the hydrogenation occurs first on the external 6-membered rings before the internal 5-membered ring as shown in Figure 5 and Figure S7 in the ESI.²⁷



Heating rate (°C/min)	Peak 1 area (mWh/mg)	Peak 2 area (mWh/mg)	Peak 1/Peak 2 area ratio
1	0.196±0.001	0.108±0.001	1.815±0.026
2	0.215±0.001	0.129±0.001	1.667±0.018
3	0.204±0.001	0.146±0.001	1.397±0.017

Figure 5 - Hydrogenation mechanism, peak area and ratio obtained from peak deconvolution by gauss fitting.

However, the peak area ratio was closer to 1.7 than 2 at low heating rate and decreased to 1.4 at high heating rate. This shift could be explained by the incomplete conversion of the 8H-NEC intermediate to 12H-NEC (DoH=70-78%). To verify this hypothesis, NEC hydrogenation at higher pressures was performed as presented in Figure 6 and Figure S8 in the ESI.



H ₂ pressure (bar)	Degree of hydrogenation	Measured hydrogenation enthalpy (kJ/mol H ₂)	Peak 1 area (mWh/mg)	Peak 2 area (mWh/mg)	Peak 1/Peak 2 area ratio
5	73%	-46.8	0.215±0.001	0.129±0.001	1.667±0.018
10	84%	-46.1	0.209±0.001	0.139±0.001	1.504±0.018
30	91%	-43.2	0.236±0.001	0.048±0.001	4.916±0.127
50	97%	-45.3	0.285±0.001		N/A

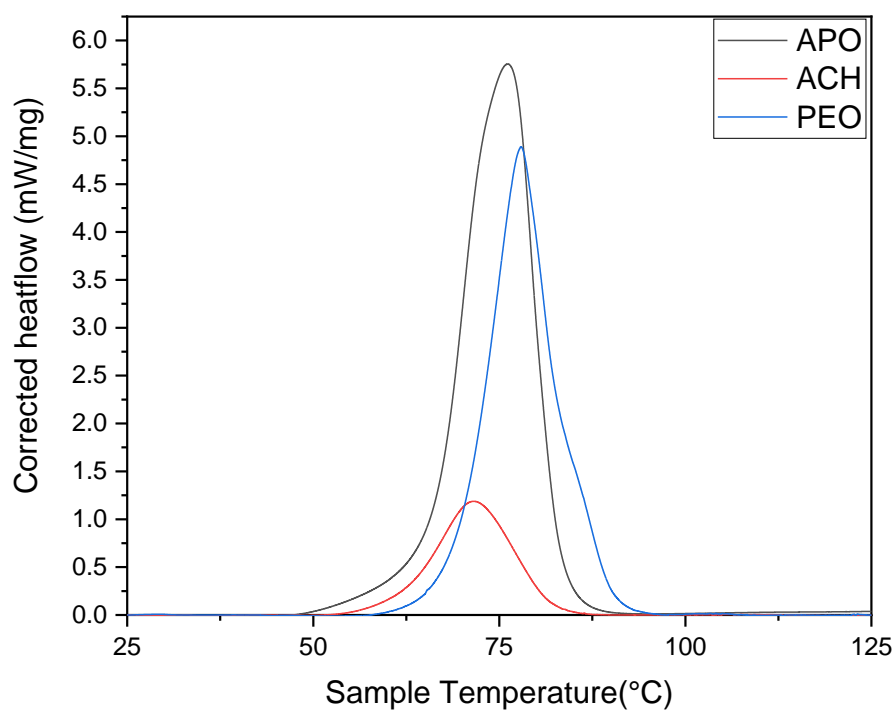
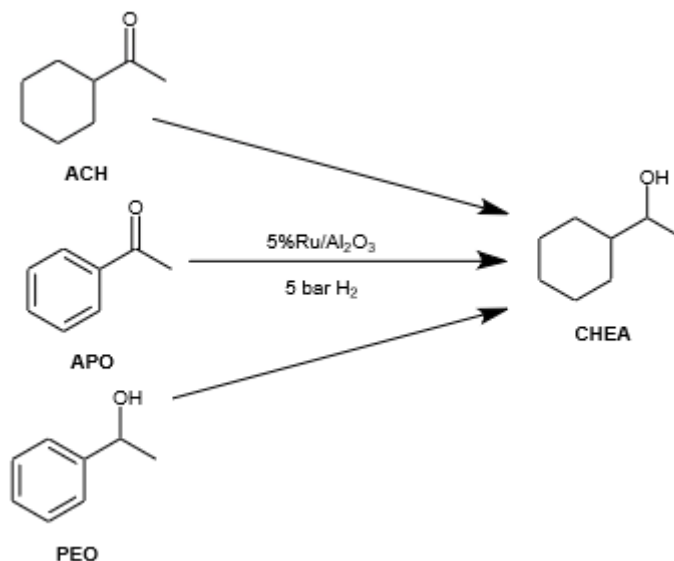
Figure 6 - Effect of the pressure on the Degree of Hydrogenation, the hydrogenation enthalpy and the peak area ratio during the hydrogenation of N-Ethylcarbazole at 2 °C/min. N/A: not applicable.

Interestingly, the peak ratio stayed stable up to 10 bar H₂, but instead of converging to 2, the peak ratio increased to roughly 5 at 30 bar and no second peak was observed at 50 bar. It is possible that, as the H₂ pressure increases, the hydrogenation kinetics would accelerate for both steps, merging them into one at higher pressures. Moreover, the peak ratio of 5 obtained at 30 bar was probably inflated due to the difficulty to deconvolute very close peaks, explaining the deviation from the theoretical value of 2. As expected, the DSC hydrogenation enthalpy was mostly constant on a wide range of pressures, indicating the limited influence of the pressure on the hydrogenation enthalpy. In conclusion, the H₂ pressure could modify the profile of the hydrogenation kinetics steps and harnessing these results might facilitate the understanding of kinetics to design more efficient hydrogenation reactors.

- d. Measure of the hydrogenation enthalpy for new LOHCs: the case of the 1-cyclohexylethanol/acetophenone (CHEA/APO) couple and its intermediates acetylcyclohexane (ACH) and 1-phenylethanol (PEO)

We previously reported the 1-cyclohexylethanol/acetophenone (CHEA/APO) couple as a potential ketone/aromatic bifunctional LOHC and described its thermodynamic profile by DFT calculations.²⁸ In this contribution, we aimed to verify the predictive power of DFT with regards

to this potential LOHC couple and in particular to estimate its accuracy with regard to the ketone and aromatic functions by using acetylcyclohexane (ACH) and 1-phenylethanol (PEO) respectively, as presented in Figure 7 and Figure S9 in the ESI.



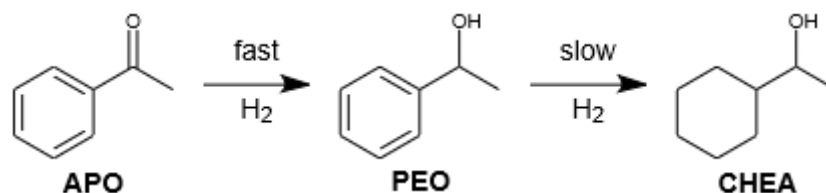
Starting material	ΔH_{hyd} by DSC (kJ/mol H ₂)	ΔH_{hyd} by DFT (kJ/mol H ₂)	DSC/DFT Relative error	Gas phase ΔH_{hyd} from the literature (kJ/mol H ₂)	Liquid phase ΔH_{hyd} from the literature (kJ/mol H ₂)
Acetophenone	-62.1±1.5	-64.9	7.5%	—	—

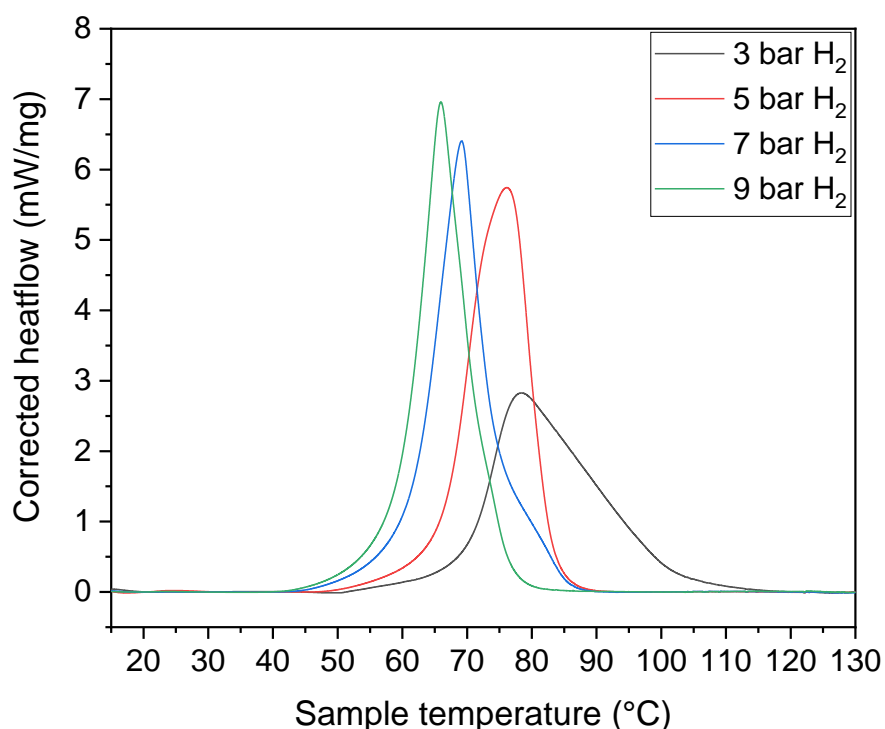
Acetylcyclohexane	-60.4±1.1	-54.1	11.6%	(Acetone) -53.8±1.5	(Acetone) -68.8±1.3
1-Phenylethanol	-64.4±2.1	-68.3	6.1%	(Toluene) -68.8±0.7	(Toluene) -67.4±0.7

Figure 7 - Comparison of the hydrogenation enthalpy (ΔH_{hyd}) obtained by DSC measurements of acetophenone (APO), acetylcyclohexane (ACH) and 1-phenylethanol (PEO) with 5%Ru/Al₂O₃ at 2 °C/min under 5 bar H₂, and their comparison with values from DFT calculations and the literature. All degree of hydrogenation were superior to 99% with less than 10% dehydration products present at the end of the reaction.

Here, APO and PEO hydrogenation enthalpies were predicted by DFT with an acceptable error below 8%. On the contrary, ACH, that represents the hydrogenation of the ketone function, exhibited an increased error of 11.6%. As it was the case for 2-OC, such variation was hypothesized to be caused by the limited accuracy of DFT calculations for intermolecular interactions happening in the liquid state. The comparison of each chemical function with the reference structures like isopropanol/acetone and methylcyclohexane/toluene allowed for the comparison of their hydrogenation enthalpy in liquid and gas phase.^{29–32} Here, the difference between the gas and liquid phases was more prominent for the isopropanol/acetone couple with a difference of 15 kJ/mol compared to the methylcyclohexane/toluene couple that exhibited a difference of only 1.4 kJ/mol. Therefore, LOHCs containing the ketone function would require a more suitable solvation model to fine-tune the liquid phase enthalpy prediction potential of DFT.

Interestingly, a two-step process was also hypothesized for this LOHC due to the presence of different chemical functions. Peak deconvolution analysis in the 3–9 bar H₂ pressure range is presented in Figure 8 and Figure S10 in the ESI. Less than 10% of dehydration were also present at the end of the reaction but no other exothermic peak (dehydration) or endothermic peak (evaporation) was observed by DSC. Moreover, reduction of the final temperature from 150 °C to 100 °C further diminished the dehydration below 5%, indicating that the measured enthalpy corresponded to the hydrogenation of APO.





H ₂ pressure (bar)	Degree of hydrogenation	Measured hydrogenation enthalpy (kJ/mol H ₂)	Peak 1 area (mWh/mg)	Peak 2 area (mWh/mg)	Peak 2/Peak 1 area ratio
3	>99% 8% dehydration	-64.2	0.087±0.001	0.371±0.001	4.264±0.062
5	>99% 9% dehydration	-61.9	0.127±0.009	0.438±0.009	3.449±0.339
7	>99% 6% dehydration	-63.1	0.196±0.001	0.391±0.001	1.995±0.015
9	>99% 7% dehydration	-61.9	0.142±0.001	0.423±0.001	2.979±0.028

Figure 8 - Effect of the pressure on the Degree of Hydrogenation and the peak area ratio during the hydrogenation of acetophenone at 2 °C/min.

Here, the two-step hydrogenation of APO was less distinguishable as no clear shoulder was present on the corrected heatflow curves. In addition, the peak asymmetry that was visible at lower pressures completely disappeared once above 5 bar H₂. Concomitantly, the peak ratio rapidly diminished from 4.3 to roughly 3, the ideal ratio value for APO. These results indicate either similar step kinetics or rapid transfer hydrogenation reaction depending on the pressure. Indeed, proton transfer could not be excluded as it was observed during the dehydrogenation of CHEA to APO at atmospheric pressure in our previous study.²⁸

e. Experimental vs computational enthalpy of Acetophenone derivatives

Over the years, numerous articles have linked the hydrogenation enthalpy value to electronic effects arising from substituents linked to aromatic structures.^{5,6,33} Here, the experimental contributions of the substituents on the hydrogenation enthalpy of acetophenone derivatives were compared with the calculated values obtained by DFT as presented in Figure 9. The

hydrogenation enthalpy of all structures was obtained by following the procedure for liquid LOHC with the exception of benzophenone (BPO) whose enthalpy was obtained by following the procedure for solid LOHC. The BPO fusion enthalpy was measured under 5 bar N₂ (18.2 kJ/mol with a peak temperature of 53.3 °C), in good agreement with the fusion enthalpy already reported in the literature (18.81 kJ/mol at 48.05 °C).³⁴

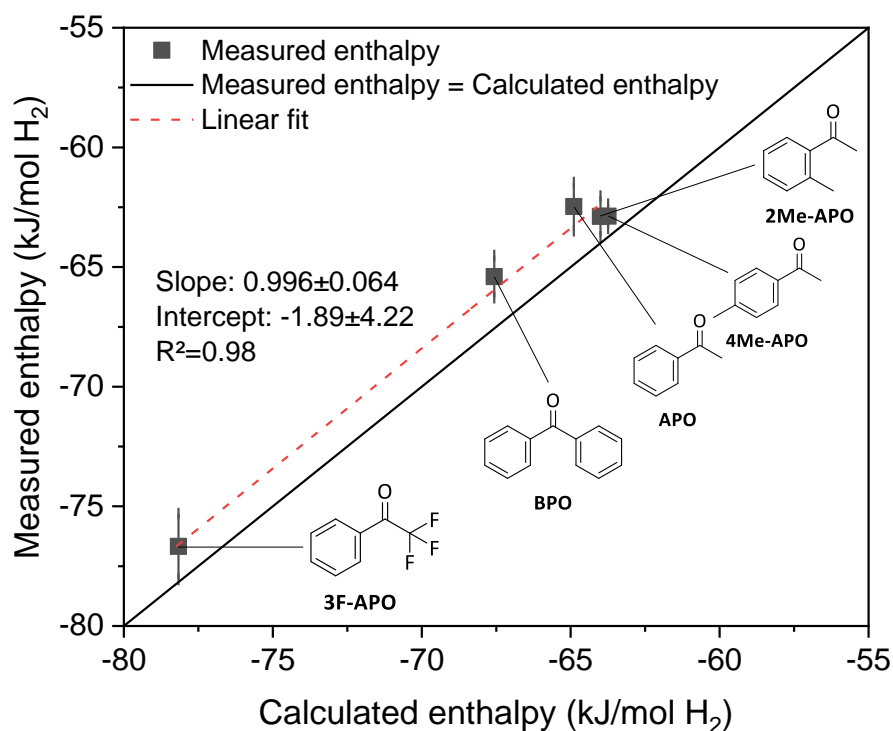
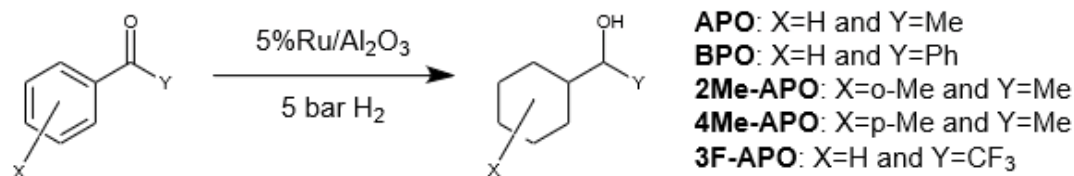
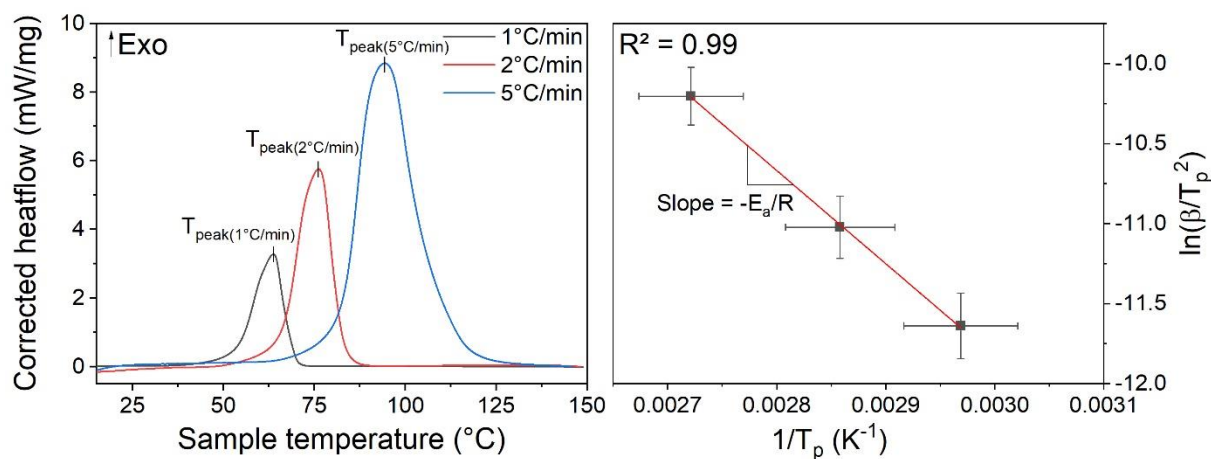


Figure 9 - Comparison of the DFT calculated and DSC measured enthalpies.

As expected, comparatively to APO, the methyl derivatives 2Me-APO and 4Me-APO exhibited a lower exothermic hydrogenation enthalpy due to donor inductive effects to the aromatic cycle while the alpha-trifluoro derivative 3F-APO had a more exothermic enthalpy due to attractive inductive effects. BPO should have exhibited less exothermic enthalpy value if the aromatic delocalization was increased. Here, a more exothermic enthalpy value indicated that aromatization did not happen, probably due to the twisted configuration of the molecule.³⁵ While the measured enthalpies closely matched the calculated enthalpies, their values were always slightly overestimated by DFT. Interestingly, all APO derivatives were aligned and a linear fit showed a slope of roughly 1, parallel to the measured=calculated curve. This result shows that the error might be attributed to similar factors for all structures. Most importantly, the intercept of the linear fitting (-1.89 ± 4.22 kJ/mol H₂) could then be used as a DFT correction factor accounting for the liquid state interactions in the case of APO derivatives. Although the number of points is limited and the intercept error is significant, this methodology provides an experimental procedure to correct the predicted enthalpy value for a specific LOHC class.

2) Activation energy measurement for various LOHCs on 5%Ru/Al₂O₃ catalyst

Activation energy (E_a) is a key parameter to study a system kinetics and to further improve design of catalysts. In our experimental conditions, only a thin liquid LOHC film was present at the catalyst surface. Moreover, no stirring was provided in the crucible, leaving all molecular movements to thermal agitation. Thus, the developed DSC system was more akin to a biphasic gas/solid system than a triphasic gas/liquid/solid system. From this consideration, we hypothesized that this system behaved similarly to metal hydride systems. Activation energy measurement for metal hydrides can be performed by following the Kissinger equation (2).³⁶ The activation energy of each studied system is presented in Figure 10.



Molecule	Activation energy (kJ/mol)	R ²
2-OC	47.4±3.0	0.99
DBT first peak	50.3±2.8	0.99
DBT second peak	46.3±2.5	0.99
NEC	48.4±6.8	0.96
APO	48.4±0.9	0.99
ACH	50.4±1.7	0.99
PEO	47.2±0.9	0.99
2Me-APO	61.3±0.8	0.99
4Me-APO	53.6±2.0	0.99
BPO	55.4±1.6	0.98
3F-APO	51.3±4.3	0.98

Figure 10 - Methodology to obtain the activation energy for each molecule. The presented heat flow values and linear regression were obtained for acetophenone.

All activation energies for the 5%Ru/Al₂O₃ catalyst ranged from 45 to 60 kJ/mol. This energy range was reported as typical activation energies for “catalytic hydrogenation processes carried out under kinetics control”.³⁷ Moreover, experiments reporting the hydrogenation of pentanal on a Ru surface indicated that these energies could be mainly linked to the H₂ adsorption activation energy on a Ru surface (48.6 kJ/mol) while the hydrogenation.³⁸ Furthermore, liquid/solid mass transfer limitations could be excluded as the activation energies were significantly higher than 10-15 kJ/mol.³⁹

Surprisingly, the activation energy for hydrogenation of the DBT external cycles was slightly higher than that of DBT internal cycle hydrogenation. However, the difference was limited and within the measurement error. Finally, the activation energies of APO and its derivatives coincided with the values reported in the literature for the partial and complete hydrogenation

of p-isobutylacetophenone with Ru/Al₂O₃ (42-57 kJ/mol).⁴⁰ The activation energy of APO was also constant in the 5-9 bar H₂ range (see Figure S11 in the ESI). In addition, steric hindrance effects were observed on the APO derivatives: 2Me-APO presented a higher activation energy than 4Me-APO, implying that the o-methyl position might disfavor the binding of the LOHC on the active site more than the p-methyl position.^{41,42} Similarly, steric hindrance due to the group in α of the ketone also increased the activation energy, suggesting that the accessibility of the ketone function was also primordial to lower the activation energy.

3) Reaction order in H₂

Determining the reaction order of a reaction is key to design a chemical process. While it can be obtained by carrying experimental plans such as modifying the reactants concentrations, the DSC methodology capitalizes on the same experimental data previously used for enthalpy measurement and activation energy to access the reaction order in H₂. Indeed, the peak asymmetry (i.e. the ratio between the difference of the endset temperature with the peak temperature and the difference of the peak temperature with the onset temperature as presented in equation (4) and Figure S16 in the ESI) is directly linked to the reaction order in H₂.³⁶ The average reaction order for each molecule is presented in Figure 11 and Figure S12 in the ESI.

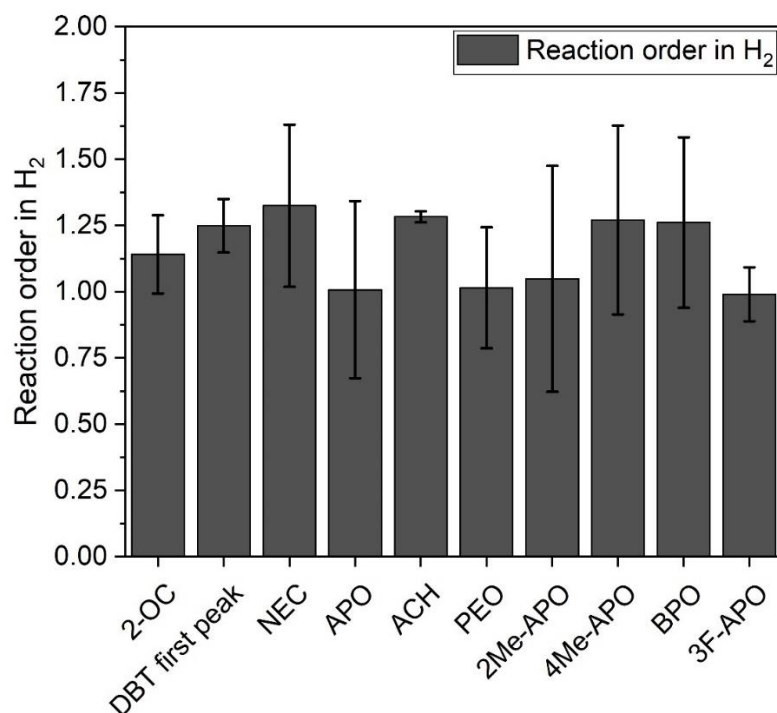


Figure 11 - Average reaction order for each studied molecule.

The reaction order in H₂ for DBT could not be fully calculated as the presence of two fused peaks limited the extraction of the peak temperatures to the first peak only (see Figure S13 in the ESI). Usually, the average reaction order in H₂ was close to 1, which was also reported for the hydrogenation of Benzene to Cyclohexane as well as NEC.⁴³⁻⁴⁵

However, as presented in Figure 12 and in Figure S14 in the ESI, a more in-depth analysis revealed that the reaction order was dependent on the heating rate with lower n values at low heating rates although n should be independent from the heating rates as described by Kissinger's theory.³⁶ These results show that the Kissinger's overall reaction order approach might not be suitable for multistep hydrogenation processes where transfer hydrogenation reactions can take place.

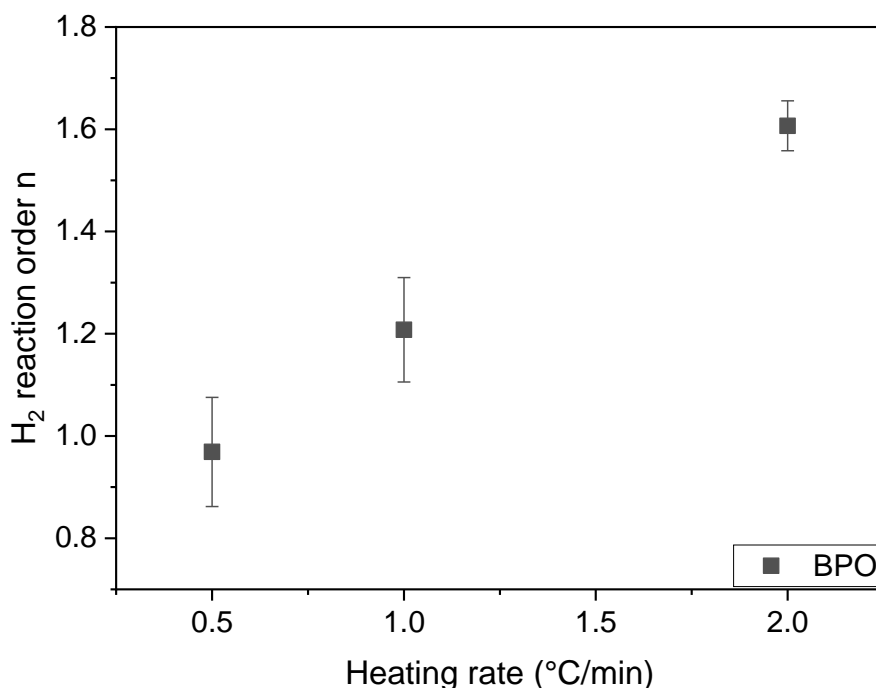


Figure 12 – Dependence of the reaction order in H₂ to the heating rate for benzophenone.

Moreover, the reaction order in H₂ was also dependent on the pressure due to the presence of two peaks at lower pressures. However, the sense of variation was different for NEC and APO, possibly due to the position of the second smaller peak. Indeed, in the case of NEC, the smaller peak induced a peak asymmetry at higher temperatures as presented in Figure 6 and Figure S8 in the ESI, while the opposite was observed for APO as presented in Figure 8 and ESI S10. Therefore, the overall sense of variation of the reaction order shift was inverted for NEC and APO as presented in Figure S14 in the ESI. Finally, considering that all double peaks could be well-fitted by a pair of symmetric gaussian curves ($R^2 > 0.99$), the relative observed asymmetry was attributed to the presence of two reactions with a reaction order of 1 in H₂.

Conclusion

Here, we reported the direct hydrogenation enthalpy measurement of well-known LOHCs (Dibenzyltoluene, N-Ethylcarbazole), molecules reported in the literature (2-Octanone) and new LOHC structures (Acetophenone and its derivatives) by Differential Scanning Calorimetry under H₂ pressure. The obtained hydrogenation enthalpies showed a good correspondence with our Density Functional Theory predictions as well as available data in the literature. Moreover, this methodology allowed to study multistep hydrogenation processes, in particular for Dibenzyltoluene, N-Ethylcarbazole and Acetophenone. It was also evidenced that transfer hydrogenation occurred during the reaction. The study of new bifunctional LOHC such as Acetophenone and its derivatives showcased the implementation of direct enthalpy measurement for rapid screening of new potential LOHC systems. In addition, a DFT correction factor for a specific LOHC class was experimentally obtained, enabling future more precise DFT predictions for similar bifunctional systems. Kinetics parameters could simultaneously be extracted. In particular, activation energies for the catalytic Ru/Al₂O₃ system were obtained in the 45-60 kJ/mol range, compatible with the H₂ adsorption on the Ru surface. Moreover, the detrimental effect of steric hinderance due to the presence and position of a methyl group on the cycle as well as groups in alpha of the carbonyl was observed. Finally, the reaction order

in H₂ for the hydrogenation was experimentally estimated to ~1 for all LOHCs. Nevertheless, the determination of the reaction order in H₂ was complicated in the case of simultaneous hydrogenation processes and showed a dependency on heating rates and H₂ pressure.

In this contribution, all experiments were performed with a 5%Ru/Al₂O₃ catalyst. Further work could be pursued with different catalysts, supports and catalyst loadings to evaluate their impact on the activation energy. More work is also required to fully understand the dependency of the reaction order in H₂ to the system parameters.

The presented results showcase the efficiency of the DSC methodology to rapidly obtain both thermodynamic and kinetic parameters for LOHC systems, facilitating the research of hydrogen storage materials.

Experimental

1.1. Materials

Acetophenone (99%, ref. A10701-1L, Lot STBH8205), 1-Phenylethanol (98%, ref. P 13800-25g, Lot SHBL4921), Benzophenone (99%, ref. B 3300-500g-A, Lot BCCF2030) and 2-Octanone (98%, ref. W280208-1KG-K, Lot STBH7791) were purchased from Sigma-Aldrich. Acetylcyclohexane (96%, ref. 11490077, Lot 10234443) was bought from Fisher-Bioblock. 4-Methylacetophenone (96%, ref. A14469, Lot 10229719) and 9-N-Ethylcarbazole (99%, ref. A11653, Lot 10218667) were purchased from Alfa-Aesar. Dibenzyltoluene Jarytherm® (isomers mixture, ref. 083549-31) was bought from Arkema. 2-Methylacetophenone (98% ref. 126160250, Lot A0419778), 2,2,2-Trifluoroacetophenone (99%, ref. 148350250, Lot A0431102) were purchased from Acros Organics.

Reduced 5wt.% Ru/Al₂O₃ was supplied by Sigma-Aldrich (ref: 439916-25g). The lot n°03116CN was used for all of the experiments related to acetophenone, acetylcyclohexane and 1-phenylethanol while the lot n°MKCQ9888 was used for the rest of the molecules.

1.2. Methods

1.2.1. Sample preparation for liquid LOHC molecules

The sample was prepared by introducing circa 25 mg of LOHC in a small DSC crucible. Control of the added LOHC weight between experiments (± 0.1 mg) was required to ensure reproducible results. Then, circa 75 mg of the Ru/Al₂O₃ catalyst was added on top of the LOHC. The DSC crucible screw pitch was coated with Cu-based grease before connection to the DSC apparatus. The system was purged under vacuum (-1 bar rel.), then under H₂ (9 bar rel.). A leak detection was operated to verify the sealing. Finally, the system was vented to 0 bar rel.

1.2.2. Sample preparation for solid/near-liquid LOHC molecules

The solid LOHC and catalyst were weighted then grounded together to form a uniform solid mixture of known composition. Then, circa 90 mg of the solid mixture was introduced in the DSC cell. Control of the added solid mixture weight between experiments (± 0.1 mg) was required to ensure reproducible results. The DSC crucible screw pitch was coated with Cu-based grease before connection to the DSC apparatus. The system was purged under vacuum (-1 bar rel.), then under H₂ (9 bar rel.). A leak detection was operated to verify the sealing. Finally, the system was vented to 0 bar rel.

To improve the contact between the LOHC and the catalyst, the solid mixture was heated up to 100 °C under 5 bar N₂ to achieve the fusion of the LOHC and its dispersion by capillarity in the pores of the catalyst. The system was then cooled to 10 °C and purged under vacuum to

remove N₂ from the system. An estimation of the fusion enthalpy of solid LOHC was obtained after performing this procedure three times.

1.2.3. Classic DSC heating program

All DSC results were obtained on a Setaram Sensys EVO DSC apparatus with dedicated gas control panel and special sample holder designed to handle 400 bar maximal pressure at 600 °C. Heat flow calibration of DSC was performed by melting reference indium compound. Starting temperature for all measurement was set to 10 °C. Then, the H₂ pressure was regulated to the chosen value (between 5 and 50 bar) with the system kept at isobaric condition during the experiment.

In a classic heating program, the DSC samples holders were heated from 10 to 150 °C at a 2 °C/min rate. Blank tests were performed under similar heating profiles.

The DSC data presented in this work had its background subtracted before being analyzed by the software Proteus.

1.2.4. Post experiment

At the end of the experiment, the DSC cell was purged under vacuum before being disconnected from the apparatus. The grease was removed with a tissue and the weight of the cell containing the reactant and the catalyst was measured. Then, the cell was cleaned with Acetone (10 mL) under sonication. The Acetone solution was filtered on a syringe filter (0.2 µm pore diameter) to remove the catalyst before GC-MS analysis (see 1.2.5). The DSC cell was sonicated three times with clean Acetone until no more catalyst was found in the Acetone solution. After drying the DSC cell with compressed air, the cleaned-up cell weight was measured to verify that no LOHC or catalyst was left in the cell.

1.2.5. GC-MS analysis

Identification and composition of the reaction crude mixtures were performed by a 7820A Agilent GC-MS (5977E MSD) with a 7693A Autosampler. The column was a 30 m, 0.25 mm diameter, 0.5 µm film HP-INNOWAX. Helium was used as the carrier gas (1 mL/min). acetophenone (APO), acetylcyclohexane (ACH), 1-cyclohexylethanol (CHEA), 1-phenylethanol (PEO), ethylbenzene (EB) and ethylcyclohexane (EC) were calibrated to obtain the response factor of the equipment. Unavailable chemicals (e.g. 2-methyl-1-cyclohexylethanol) were supposed to have a response factor similar to that of already calibrated akin or related products (e.g. 1-cyclohexylethanol). To perform the analysis, 0.5 mL of the acetone solution were diluted with 1.5 mL of an acetonitrile solution containing 0.25%vol. 3-octanone as an internal standard. A split ratio of 1:20 was applied to the 1 µL injection. The heat program was: initial oven temperature 50 °C, final oven temperature 260 °C for 7 min, program rate 45 °C/min.

1.2.6. Definition of the Degree of Hydrogenation (DoH)

The degree of hydrogenation is used during the hydrogenation to quantify the amount of H₂ stored by the system. Hydrogenation coefficients detailed in the Figure S15 in the ESI are used to qualify the amount of hydrogen stored by the hydrogenation of the APO system. For the CHEA/APO couple, the DoH is calculated by the equation (1):

$$DoH = \frac{\text{Quantity of } H_2 \text{ stored}}{\text{Maximum theoretical } H_2 \text{ amount}} = \frac{\sum_i (C_{H,i} \times \text{mol}\%_i)}{4} \quad (1)$$

1.2.7. Activation energy

The activation energy in a dynamic system was obtained by using the Kissinger equation that is derived from Arrhenius' law as presented by the equation (2).³⁶

$$\ln\left(\frac{\beta}{T_p^2}\right) = -\frac{E_a}{RT_p} + \alpha \quad (2)$$

With β the heating rate (K/min), T_p the peak temperature (K), E_a the activation energy (J/mol), R the ideal gas constant (8.314 J/K/mol) and α the integration constant.

1.2.8. Reaction order in H₂

The reaction order in H₂ was obtained by first supposing that the reaction was similar to a "solid+ gas → solid" type reaction with its reaction rate given by the equation (3).

$$r = k[H_2]^n[LOHC]^x \quad (3)$$

With r the reaction rate, k the rate constant, n the reaction order in H₂ and x the reaction order in LOHC. Analytical development linking the peak shape to the reaction order in H₂ was performed by Kissinger as presented in Figure S16 in the ESI.³⁶ The reaction order in H₂ is calculated by the equation (4).

$$n = 1.26S^{0.5} \text{ with } S = \frac{a}{b} = \frac{T_{\text{endset}} - T_{\text{peak}}}{T_{\text{peak}} - T_{\text{onset}}} \quad (4)$$

The peak, onset and endset temperatures were obtained by the analysis with the software Origin. The T_{onset} and T_{endset} values are found at the intersection between the baseline and the tangents at the peak inflexion points.

1.2.9. DFT

All computations have been performed with the Gaussian 16 Rev C.01 suite, using the hybrid meta-GGA functional M06-2X and the basis set 6-311+G(2d,p) for elements. Such parameters are known to predict accurately the thermochemistry of main-group compounds in the ground-state as well as polyenes systems.⁴⁶ Each structure is solvated in Acetophenone using the SMD model which is recommended to compute thermochemical parameters. Frequency calculations were performed on the optimized structures using the same parameters; all structures were verified to possess no imaginary frequencies. All computed structures are grouped in Figure S17 in the ESI.

Acknowledgments

This work was supported by the CEA, the CNRS, the University Paris-Saclay, DARI (HPC Computing time on Irene, grant no. AD010806494R1), the European Research Council (ERC Consolidator Grant Agreement no. 818260) and the European project funding from the Fuel Cells and Hydrogen 2 Joint Undertaking under grant agreement No 101007223.

References

- (1) Caglar, B.; Açıkkalp, E.; Altuntas, O.; Palmero-Marrero, A. I.; Zairov, R.; Borge-Diez, D. Exergetic Assessment of an Solar Powered Stand-Alone System Using Liquid Organic Hydrogen Carrier for Energy Storage. *Solar Energy* **2023**, *264*, 112041. <https://doi.org/10.1016/j.solener.2023.112041>.
- (2) Rao, P. C.; Yoon, M. Potential Liquid-Organic Hydrogen Carrier (LOHC) Systems: A Review on Recent Progress. *Energies* **2020**, *13* (22), 6040. <https://doi.org/10.3390/en13226040>.

- (3) Grimaldo-Guerrero, J.-W.; Barcelo, J. D. la H.; Rivera-Pacheco, D.; Ramos-Barrera, L.; Martinez-Palacio, U. A Review of History, Production and Storage of Hydrogen. *JESTR* **2021**, *14* (5), 121–134. <https://doi.org/10.25103/jestr.145.14>.
- (4) Niermann, M.; Beckendorff, A.; Kaltschmitt, M.; Bonhoff, K. Liquid Organic Hydrogen Carrier (LOHC) – Assessment Based on Chemical and Economic Properties. *International Journal of Hydrogen Energy* **2019**, *44* (13), 6631–6654. <https://doi.org/10.1016/j.ijhydene.2019.01.199>.
- (5) Cooper, A. C. *Design and Development of New Carbon-Based Sorbent Systems for an Effective Containment of Hydrogen*; 86-377-P; Air Products and Chemicals, Inc., 2012. <https://doi.org/10.2172/1039432>.
- (6) Clot, E.; Eisenstein, O.; H. Crabtree, R. Computational Structure–Activity Relationships in H₂ Storage: How Placement of N Atoms Affects Release Temperatures in Organic Liquid Storage Materials. *Chemical Communications* **2007**, *0* (22), 2231–2233. <https://doi.org/10.1039/B705037B>.
- (7) Zaitsau, D. H.; Emel'yanenko, V. N.; Pimerzin, A. A.; Verevkin, S. P. Benchmark Properties of Biphenyl as a Liquid Organic Hydrogen Carrier: Evaluation of Thermochemical Data with Complementary Experimental and Computational Methods. *The Journal of Chemical Thermodynamics* **2018**, *122*, 1–12. <https://doi.org/10.1016/j.jct.2018.02.025>.
- (8) LeBlond, C.; Wang, J.; Larsen, R. D.; Orella, C. J.; Forman, A. L.; Landau, R. N.; Laquidara, J.; Sowa, J. R.; Blackmond, D. G.; Sun, Y.-K. Reaction Calorimetry as an In-Situ Kinetic Tool for Characterizing Complex Reactions. *Thermochimica Acta* **1996**, *289* (2), 189–207. [https://doi.org/10.1016/S0040-6031\(96\)03072-9](https://doi.org/10.1016/S0040-6031(96)03072-9).
- (9) Landau, R. N.; Singh, U.; Gortsema, F.; Sun, Y. K.; Gomolka, S. C.; Lam, T.; Futran, M.; Blackmond, D. G. A Reaction Calorimetric Investigation of the Hydrogenation of a Substituted Pyrazine. *Journal of Catalysis* **1995**, *157* (1), 201–208. <https://doi.org/10.1006/jcat.1995.1280>.
- (10) Emel'yanenko, V. N.; Zaitsau, D. H.; Pimerzin, A. A.; Verevkin, S. P. Benchmark Properties of Diphenyl Oxide as a Potential Liquid Organic Hydrogen Carrier: Evaluation of Thermochemical Data with Complementary Experimental and Computational Methods. *The Journal of Chemical Thermodynamics* **2018**, *125*, 149–158. <https://doi.org/10.1016/j.jct.2018.05.021>.
- (11) Safronov, S. P.; Vostrikov, S. V.; Samarov, A. A.; Verevkin, S. P. Reversible Storage and Release of Hydrogen with LOHC: Evaluation of Thermochemical Data for Methyl-Quinolines with Complementary Experimental and Computational Methods. *Fuel* **2022**, *317*, 123501. <https://doi.org/10.1016/j.fuel.2022.123501>.
- (12) Selvam, P. K.; Muthukumar, P.; Linder, M.; Mertz, R.; Kulenovic, R. Measurement of Thermochemical Properties of Some Metal Hydrides – Titanium (Ti), Misch Metal (Mm) and Lanthanum (La) Based Alloys. *International Journal of Hydrogen Energy* **2013**, *38* (13), 5288–5301. <https://doi.org/10.1016/j.ijhydene.2013.02.009>.
- (13) Bohmhammel, K.; Christ, B.; Wolf, G. Kinetic Investigations on the Basis of Isothermal DSC Measurements of Hydrogenation and Dehydrogenation of Magnesium hydride1Presented at the Twelfth Ulm-Freiberg Conference, Freiberg, Germany, 19–21 March 19971. *Thermochimica Acta* **1998**, *310* (1), 167–171. [https://doi.org/10.1016/S0040-6031\(97\)00392-4](https://doi.org/10.1016/S0040-6031(97)00392-4).
- (14) Hirata, T. Pressure DSC Study of the Hydrogenation and Dehydrogenation of Some Intermetallic Compounds Mg₂Ni. *International Journal of Hydrogen Energy* **1984**, *9* (10), 855–859. [https://doi.org/10.1016/0360-3199\(84\)90142-3](https://doi.org/10.1016/0360-3199(84)90142-3).
- (15) Anastasopol, A.; Pfeiffer, T. V.; Middelkoop, J.; Lafont, U.; Canales-Perez, R. J.; Schmidt-Ott, A.; Mulder, F. M.; Eijt, S. W. H. Reduced Enthalpy of Metal Hydride Formation for Mg–Ti Nanocomposites Produced by Spark Discharge Generation. *J. Am. Chem. Soc.* **2013**, *135* (21), 7891–7900. <https://doi.org/10.1021/ja3123416>.
- (16) Sheppard, D. A.; Paskevicius, M.; Javadian, P.; Davies, I. J.; Buckley, C. E. Methods for Accurate High-Temperature Sieverts-Type Hydrogen Measurements of Metal Hydrides.

- (17) Flanagan, T. B.; Clewley, J. D. Hysteresis in Metal Hydrides. *Journal of the Less Common Metals* **1982**, *83* (1), 127–141. [https://doi.org/10.1016/0022-5088\(82\)90176-X](https://doi.org/10.1016/0022-5088(82)90176-X).
- (18) Ulmer, U.; Cholewa, M.; Diemant, T.; Bonatto Minella, C.; Dittmeyer, R.; Behm, R. J.; Fichtner, M. Thermochemical Energy Storage through De/Hydrogenation of Organic Liquids: Reactions of Organic Liquids on Metal Hydrides. *ACS Appl. Mater. Interfaces* **2016**, *8* (22), 13993–14003. <https://doi.org/10.1021/acsami.6b05537>.
- (19) Stoessel, F. Experimental Study of Thermal Hazards during the Hydrogenation of Aromatic Nitro Compounds. *Journal of Loss Prevention in the Process Industries* **1993**, *6* (2), 79–85. [https://doi.org/10.1016/0950-4230\(93\)90004-H](https://doi.org/10.1016/0950-4230(93)90004-H).
- (20) Cubberley, A. H.; Mueller, M. B. Equilibrium Studies on the Dehydrogenation of Primary and Secondary Alcohols. I. 2-Butanol, 2-Octanol, Cyclopentanol and Benzyl Alcohol. *J. Am. Chem. Soc.* **1946**, *68* (7), 1149–1151. <https://doi.org/10.1021/ja01211a003>.
- (21) Chickos, J. S.; Hosseini, S.; Hesse, D. G. Determination of Vaporization Enthalpies of Simple Organic Molecules by Correlations of Changes in Gas Chromatographic Net Retention Times. *Thermochimica Acta* **1995**, *249*, 41–62. [https://doi.org/10.1016/0040-6031\(95\)90670-3](https://doi.org/10.1016/0040-6031(95)90670-3).
- (22) Verevkin, S. P.; Schick, C. Vapour Pressures and Heat Capacity Measurements on the C7–C9 Secondary Aliphatic Alcohols. *The Journal of Chemical Thermodynamics* **2007**, *39* (5), 758–766. <https://doi.org/10.1016/j.jct.2006.10.007>.
- (23) Müller, K.; Stark, K.; Emel'yanenko, V. N.; Varfolomeev, M. A.; Zaitsau, D. H.; Shoifet, E.; Schick, C.; Verevkin, S. P.; Arlt, W. Liquid Organic Hydrogen Carriers: Thermophysical and Thermochemical Studies of Benzyl- and Dibenzyl-Toluene Derivatives. *Ind. Eng. Chem. Res.* **2015**, *54* (32), 7967–7976. <https://doi.org/10.1021/acs.iecr.5b01840>.
- (24) Do, G.; Preuster, P.; Aslam, R.; Bösmann, A.; Müller, K.; Arlt, W.; Wasserscheid, P. Hydrogenation of the Liquid Organic Hydrogen Carrier Compound Dibenzyltoluene – Reaction Pathway Determination by ¹H NMR Spectroscopy. *Reaction Chemistry & Engineering* **2016**, *1* (3), 313–320. <https://doi.org/10.1039/C5RE00080G>.
- (25) Verevkin, S. P.; Emel'yanenko, V. N.; Pimerzin, A. A.; Vishnevskaya, E. E. Thermodynamic Analysis of Strain in the Five-Membered Oxygen and Nitrogen Heterocyclic Compounds. *J. Phys. Chem. A* **2011**, *115* (10), 1992–2004. <https://doi.org/10.1021/jp1090526>.
- (26) Stark, K.; Keil, P.; Schug, S.; Müller, K.; Wasserscheid, P.; Arlt, W. Melting Points of Potential Liquid Organic Hydrogen Carrier Systems Consisting of N-Alkylcarbazoles. *J. Chem. Eng. Data* **2016**, *61* (4), 1441–1448. <https://doi.org/10.1021/acs.jced.5b00679>.
- (27) Sotoodeh, F.; Smith, K. J. Kinetics of Hydrogen Uptake and Release from Heteroaromatic Compounds for Hydrogen Storage. *Ind. Eng. Chem. Res.* **2010**, *49* (3), 1018–1026. <https://doi.org/10.1021/ie9007002>.
- (28) D'Ambra, F.; Levy, J.; Hajiyev, P.; Cantat, T.; Gébel, G.; Faucheux, V.; Nicolas, E. Evaluation of Acetophenone as a Novel Alcohol-Cycloalkane Bifunctional Liquid Organic Hydrogen Carrier (LOHC). *International Journal of Hydrogen Energy* **2023**. <https://doi.org/10.1016/j.ijhydene.2023.05.024>.
- (29) Wiberg, K. B.; Crocker, L. S.; Morgan, K. M. Thermochemical Studies of Carbonyl Compounds. 5. Enthalpies of Reduction of Carbonyl Groups. *J. Am. Chem. Soc.* **1991**, *113* (9), 3447–3450. <https://doi.org/10.1021/ja00009a033>.
- (30) Snelson, A.; Skinner, H. A. Heats of Combustion: Sec-Propanol, 1,4-Dioxan, 1,3-Dioxan and Tetrahydropyran. *Trans. Faraday Soc.* **1961**, *57*, 2125. <https://doi.org/10.1039/TF9615702125>.
- (31) Roux, M. V.; Temprado, M.; Chickos, J. S.; Nagano, Y. Critically Evaluated Thermochemical Properties of Polycyclic Aromatic Hydrocarbons. *Journal of Physical and Chemical Reference Data* **2008**, *37* (4), 1855–1996. <https://doi.org/10.1063/1.2955570>.
- (32) Prosen, E. J.; Johnson, W. H.; Rossini, F. D. Heats of Formation and Combustion of the Normal Alkylcyclopentanes and Cyclohexanes and the Increment per CH₂ Group for

- Several Homologous Series of Hydrocarbons. *J. RES. NATL. BUR. STAN.* **1946**, 37 (1), 51. <https://doi.org/10.6028/jres.037.031>.
- (33) Müller, K.; Völkl, J.; Arlt, W. Thermodynamic Evaluation of Potential Organic Hydrogen Carriers. *Energy Technology* **2013**, 1 (1), 20–24. <https://doi.org/10.1002/ente.201200045>.
- (34) Chirico, R. D.; Knipmeyer, S. E.; Steele, W. V. Heat Capacities, Enthalpy Increments, and Derived Thermodynamic Functions for Benzophenone between the Temperatures 5K and 440K. *The Journal of Chemical Thermodynamics* **2002**, 34 (11), 1885–1895. [https://doi.org/10.1016/S0021-9614\(02\)00261-6](https://doi.org/10.1016/S0021-9614(02)00261-6).
- (35) Ibeji, C. U.; Adegboyega, J.; Okagu, O. D.; Adeleke, B. B. Nature of Ground State of Benzophenone and Some of Its Substituted Derivatives: Experimental and DFT Study. *Journal of Applied Sciences* **2016**, 16 (11), 504–516. <https://doi.org/10.3923/jas.2016.504.516>.
- (36) Kissinger, H. E. Reaction Kinetics in Differential Thermal Analysis. *Anal. Chem.* **1957**, 29 (11), 1702–1706. <https://doi.org/10.1021/ac60131a045>.
- (37) Neri, G.; Bonaccorsi, L.; Galvagno, S. Kinetic Analysis of Cinnamaldehyde Hydrogenation over Alumina-Supported Ruthenium Catalysts. *Ind. Eng. Chem. Res.* **1997**, 36 (9), 3554–3562. <https://doi.org/10.1021/ie9607457>.
- (38) Vaidya, P. D.; Mahajani, V. V. Kinetics of Liquid-Phase Hydrogenation of n-Valeraldehyde to n-Amyl Alcohol over a Ru/Al₂O₃ Catalyst. *Chemical Engineering Science* **2005**, 60 (7), 1881–1887. <https://doi.org/10.1016/j.ces.2004.11.023>.
- (39) Zhao, Y.; Zhou, J.; Zhang, J.; Li, D.; Wang, S. Selective Hydrogenation of Benzene to Cyclohexene on a Ru/Al₂O₃/Cordierite Monolithic Catalyst: Effect of Mass Transfer on the Catalytic Performance. *Ind. Eng. Chem. Res.* **2008**, 47 (14), 4641–4647. <https://doi.org/10.1021/ie071574g>.
- (40) Mathew, S. P.; Rajasekharam, M. V.; Chaudhari, R. V. Hydrogenation of P-Isobutyl Acetophenone Using a Ru/Al₂O₃ Catalyst: Reaction Kinetics and Modelling of a Semi-Batch Slurry Reactor. *Catalysis Today* **1999**, 49 (1), 49–56. [https://doi.org/10.1016/S0920-5861\(98\)00407-6](https://doi.org/10.1016/S0920-5861(98)00407-6).
- (41) Toppinen, S.; Rantakylä, T.-K.; Salmi, T.; Aittamaa, J. Kinetics of the Liquid Phase Hydrogenation of Di- and Trisubstituted Alkylbenzenes over a Nickel Catalyst. *Ind. Eng. Chem. Res.* **1996**, 35 (12), 4424–4433. <https://doi.org/10.1021/ie950636c>.
- (42) Stanislaus, A.; Cooper, B. H. Aromatic Hydrogenation Catalysis: A Review. *Catalysis Reviews* **1994**, 36 (1), 75–123. <https://doi.org/10.1080/01614949408013921>.
- (43) Liu, H.; Fang, R.; Li, Z.; Li, Y. Solventless Hydrogenation of Benzene to Cyclohexane over a Heterogeneous Ru–Pt Bimetallic Catalyst. *Chemical Engineering Science* **2015**, 122, 350–359. <https://doi.org/10.1016/j.ces.2014.09.050>.
- (44) Wan, C.; An, Y.; Xu, G.; Kong, W. Study of Catalytic Hydrogenation of N-Ethylcarbazole over Ruthenium Catalyst. *International Journal of Hydrogen Energy* **2012**, 37 (17), 13092–13096. <https://doi.org/10.1016/j.ijhydene.2012.04.123>.
- (45) Gambini, M.; Guarnaccia, F.; Di Vona, M. L.; Manno, M.; Vellini, M. Liquid Organic Hydrogen Carriers: Development of a Thermodynamic and Kinetic Model for the Assessment of Hydrogenation and Dehydrogenation Processes. *International Journal of Hydrogen Energy* **2022**. <https://doi.org/10.1016/j.ijhydene.2022.06.120>.
- (46) Zhao, Y.; Truhlar, D. G. The M06 Suite of Density Functionals for Main Group Thermochemistry, Thermochemical Kinetics, Noncovalent Interactions, Excited States, and Transition Elements: Two New Functionals and Systematic Testing of Four M06-Class Functionals and 12 Other Functionals. *Theor Chem Account* **2008**, 120 (1), 215–241. <https://doi.org/10.1007/s00214-007-0310-x>.